2009 American Control Conference
Hyatt Regency Riverfront, St. Louis, MO, USA
June 10-12, 2009



# Iterative Learning Control Using a Basis Signal Library

David J. Hoelzle, *Student Member, IEEE*, Andrew G. Alleyne, *Senior Member, IEEE*, and Amy J. Wagoner Johnson

***Abstract*—There are a vast number of manufacturing applications that are repetitive in nature and therefore can benefit from Iterative Learning Control (ILC) algorithms. However, some of these applications are unfit for continuous open loop signal updates from ILC either because the complete manufacturing cycle includes abrupt transitions in system dynamics or is prohibitively long for efficient implementation. This paper explores a method to control one such system, Micro Robotic Deposition (μRD), using ILC as an open loop control signal identification technique. Instead of continuously updating the ILC control signal for the complete operation, we exploit the characteristic that all μRD cycles are a sequence of a few basis tasks and only these basis tasks are learned. Control signals for these basis tasks build a library of basis signals, which can then be appropriately sequenced as the control signal for the complete manufacturing cycle. This paper introduces a method to build this basis signal library and extract and coordinate the signals depending on predefined μRD operations and material used as specified by numerically controlled machine language. The methods applied to μRD display the ability to drastically improve end product quality with a significantly shortened signal identification process.**

## I. Introduction

ITERATIVE Learning Control (ILC) is a control algorithm that has been applied to systems that have repeated reference trajectories, identical initial conditions, and dwells in actuation between iterations[1]. The ILC algorithm uses information recorded from previous input and error signals to iteratively modify the open loop control signal. The open loop signal can either be used alone in open loop stable systems or in conjunction with feedback control[2], utilizing the noncausal nature of ILC to augment the causal nature of feedback control. With properly chosen algorithm parameters, ILC converges to an open loop signal that compensates for uncertainties that detract from system performance, notably unmodeled dynamics and repeated disturbances.

Typically, ILC is implemented as a continuously active algorithm. The dynamics of the system can be time varying provided that the changes in dynamics are not abrupt, therefore correlating with previous iterations. The standard system tracks a short duration trajectory, ensuring that the storage and calculation of updated signals is computationally efficient[3]. However, there are many systems, particularly in manufacturing, where abrupt changes in dynamics do occur, such as when a robot lifts a heavy part. Additionally, complete operations can be on the order of minutes, preventing the implementation of computationally intensive algorithms such as those utilizing lifted system analysis[4] and non-traditional sensors such as machine vision[5]. Fortunately, many manufacturing operations consist of a few basis tasks sequenced appropriately to complete the intended operation. Instead of applying ILC to the complete trajectory, a more computational and time efficient method is to learn the shorter basis tasks and then select the corresponding input signal, termed basis signal, as needed to complete the entire operation. Systems that are appropriate for this implementation must be appropriate for ILC[1] and satisfy the following assumptions:

*Assumptions:*

1) Repetition of basis tasks in an operation
2) Time invariant dynamics within a task
3) Existence a bijective map between basis signals and basis tasks
4) Approximate basis signal continuity at the transition between adjacent basis tasks

One such system is Micro Robotic Deposition (μRD)[6]. μRD is a rapid prototyping process in which a colloidal ink is extruded through a nozzle in a predefined trajectory to build three-dimensional structures, Fig. 1. Structures are built in a layer-by-layer fashion, similar to the more well-established Fused Deposition Modeling[7], except that a ceramic or polymeric ink is used rather than a polymer melt. In the μRD community, there is a demand for advanced multi-material structures such as near-net shape structures, structures with embedded sensors, and structures with multiple domains of different material properties[8]. Common to each of these structures is the requirement for precise modulation of material flowrate so that material transitions are both well connected (no unintended material gaps) and within tolerance. Fundamental limitations of the system dynamics prevent precise flowrate modulation by simple on-off control schemes[9]. ILC has been shown as a successful flowrate modulation technique in [5], however [5] focused on a complete build trajectory. Typically in μRD, different materials vary significantly in viscosity[10]

Manuscript received March 16, 2009. This work was supported in part by NSF Grants DMI-0328162 and DMI-0140466.

Andrew G. Alleyne is with the Mechanical Science and Engineering Department at the University of Illinois at Urbana-Champaign, Urbana, IL 61801 USA (phone: 217-244-9993; fax: 217-244-6534; email: alleyne@illinois.edu).

David J. Hoelzle is with the Mechanical Science and Engineering Department at the University of Illinois at Urbana-Champaign, Urbana, IL 61801 USA (email: hoelzle2@illnois.edu).

Amy J. Wagoner Johnson is with the Mechanical Science and Engineering Department at the University of Illinois at Urbana-Champaign, Urbana, IL 61801 USA (email: ajwj@illinois.edu).

and build times are on the order of minutes. Therefore, this previously developed technology must be modified to make the flowrate modulation for the complete build cycle feasible.

All structures built by μRD are built in a sequence of basis tasks, termed here as *Start*, *Stop*, *Corner*, *Steady-State*, and *No-Flow*. Therefore, the correct input signal to build any structure in μRD is a concatenation of basis signals applied at the correct location in the build cycle. Basis signals are learned in a fixed training routine that contains the set of basis tasks. Learned signals are stored in a database, termed here as the basis signal library, which is indexed and extracted by their associative basis task, material, and nozzle size. The extraction is dictated by logic applied to set of commands defining the structure architecture (e.g. G-Code).

Since the ILC algorithm is applied to a fixed training trajectory, the same conditions for boundedness of trajectories and stability that apply to ILC apply to this implementation[1]. However, in any system, there will be hysteresis effects and signal discontinuities at the transitions between basis input signals when applied to a trajectory that is not the training trajectory. Consequently system performance is sacrificed for gains in modularity. This implementation of ILC can be extended to applications beyond μRD. For instance, a pick-and-place robot manipulating objects on an assembly line will have different dynamics depending on the load[11]. Tasks such as linear moves and end effecter moves can be learned in both the load and no-load scenarios and used accordingly.

This paper explores the idea of identifying basis signals through a training routine and extracting them to build entire structures with a multi-material μRD system. The μRD system used is described in Section II. The basis signal identification technique is described in Section III, detailing the training routine, signal learning, segmentation into individual basis signals, and construction of a signal library. Section IV describes the logic employed to extract the appropriate basis signal and provides a simple example. Section V shows this method's utility in building structures with advanced architectures. Section VI follows with concluding statements.

## II. System Description

This research is applied to a multi-material μRD system. System components and functions will be described in the following sections.

### A. XYZ Gantry System

Position of the deposition head is controlled by an XYZ gantry system as described in [12]. The gantry system has approximately 20 times the bandwidth of the extrusion systems and therefore we only consider the systems with the dominant time scale, which are the extrusion systems, for ILC application.

### B. Multi-Material Deposition Head

The deposition system mounted to the XYZ gantry system is a prototype multi-material deposition head. The head contains four individual extrusion systems oriented in a rotary array, see Fig. 1a, however the technology developed here extends to more than four extrusion systems. Each individual extrusion system consists of a motor and lead screw assembly which linearly translates a plunger, which in turn applies pressure to the ink reservoir to extrude the ink, see the schematic in Fig. 1b. An individual extrusion system is selected by rotating that system into the 'active' position. The rotational system is locked into place during deposition of a material by a solenoid and locking pin mechanism. The entire system is oriented at a slight angle (2°) from parallel with the deposition substrate to provide clearance between non-active extrusion systems and the structure being fabricated.

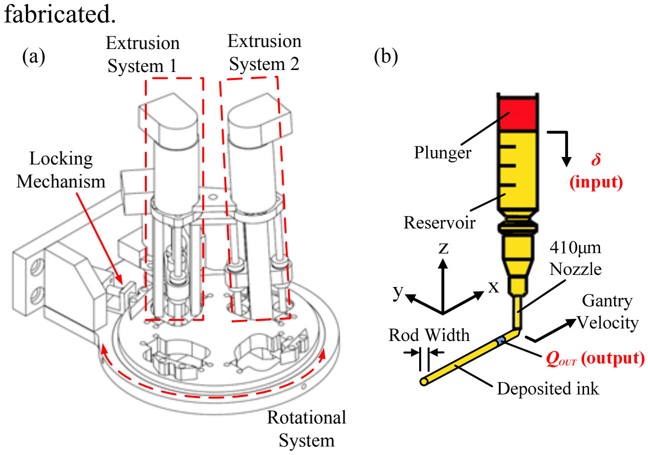


Fig. 1. Multi-Material Deposition Head. (a) Drawing of complete system. The Multi-Material Deposition Head is a rotary array of four individual extrusion systems. Extrusion systems 3 and 4 are removed for clarity. The rotational system positions the correct extrusion system into the 'active' position and is locked in place during deposition. (b) Schematic of an individual extrusion system. Plunger displacement (input) applies pressure to a reservoir of ink which in turn extrudes ink (output) through the nozzle.

The material extrusion systems, diagramed in Fig. 1b, are single-input single-output (SISO) systems where the input, $u(k)$, is the plunger displacement and the output, $y(k)$, is the material volumetric flowrate out. The extrusion system, denoted by operator $H$, is a function of build material, $M$, and nozzle size, $N$, Fig. 2. $H$ is bounded-input bounded-output (BIBO) stable[5] and is assumed to be time-invariant here. The subscript $i$ denotes the basis task index (e.g. $u_1(k)$ is basis signal number 1).

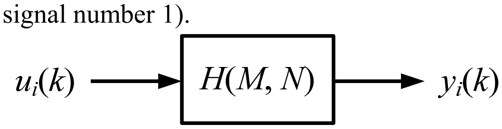


Fig. 2. Block diagram of the material extrusion system in μRD. SISO system $H(M, N)$ is BIBO stable and assumed to be time invariant.

The extrusion system, $H(M, N)$, is nominally described by a first order transfer function relating the volumetric flowrate through the syringe nozzle and the plunger displacement, equation (1). (1) is derived in [5] and in similar systems[13,14].

$$\frac{Q_{out}}{\dot{\delta}}(s) = \frac{K}{\tau s + 1} \tag{1}$$

Two different operating modes are considered, extruding either Material A or Material B but with the same nozzle size, where Materials A and B have different fluid viscosities and therefore exhibit different system dynamics, $H_A$ and $H_B$. First order parameters $K$ and $\tau$ for systems $H_A$ and $H_B$, identified by a downward step input (not shown), are given in Table I. Noticeable in the nominal system results are the slow time constants that prevents simple on-off control from effectively modulating flowrate. Additionally, Material B has a higher viscosity than Material A, realized in the difference in time constants.

TABLE I
NOMINAL SYSTEM PARAMETERS

| Parameter | $H_A$ | $H_B$ |
|---|---|---|
| K | 1.08 | 0.89 |
| τ (s) | 2.7 | 4.5 |

### C. *Machine Vision System*

Material flowrate is measured by a machine vision system. An in depth description of the machine vision system can be found in [5] and [15]. Briefly, a CCD video camera is mounted to the XYZ gantry system and focused at the exit of syringe nozzle. Video of each deposition trial is recorded and flowrate is calculated based on information known about the cross-sectional area of the extruded ink and the gantry velocity.

## III. BASIS SIGNAL IDENTIFICATION

### A. *Signal Identification*

Basis signals for each of the basis task for μRD, *Start*, *Stop*, *Corner*, *Steady-State*, and *No-Flow*, are identified in a training routine.

ILC algorithm (2) is applied to a training reference for systems $H_A$ and $H_B$. The training reference, reference signal in Fig. 3, is a pulse signal with a momentary pause in the pulsed region. The rising and falling steps are representative of the *Start* and *Stop* basis signals, respectively. The momentary pause in gantry velocity during the pulsed region simulates the gantry trajectory during a *Corner* basis signal. During a *Corner* basis signal, it is desirable to maintain a constant flowrate despite the decrease in gantry velocity. Here, a *Corner* is simulated by proceeding in a straight line, instead of actually changing direction, to make flowrate measurement easier.

$$u_{j+1}(k) = Q(q)\left(u_j(k) + L(q)e_j(k)\right) \tag{2}$$

Learning filter $L(q)$ is a model inversion filter, $L(q) = k_p \hat{P}(q)^{-1}$, where $k_p$ = 0.25 and $\hat{P}(q)$ is the discrete-time version (1) of with a fast zero added to the numerator to make the inversion proper. Q-filter, $Q(q)$, is a second-order lowpass Butterworth filter with a bandwidth of 3 Hz.

Results from ILC algorithm (2) applied to the training reference signal are shown in Fig. 3. Both systems drastically improve reference signal tracking at high iterations, approximating the training reference signal. Units are expressed in mm$^3$/mm because it is critical to control the volume of material extruded per linear travel of the Multi-Material Deposition Head. Root mean squared (RMS) error decreases to less than 20% the RMS of iteration 0 at the most accurate iteration for both systems, Fig. 4.

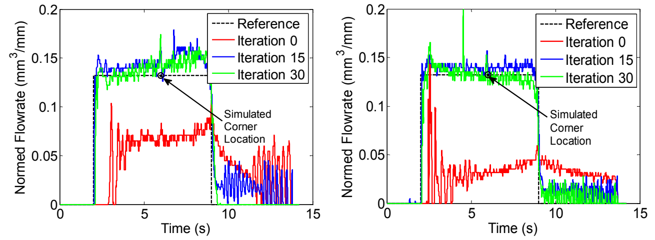

Fig. 3. Normalized flowrate response to the training reference at iterations 0, 15, and 30 for system $H_A$ (left) and $H_B$ (right).

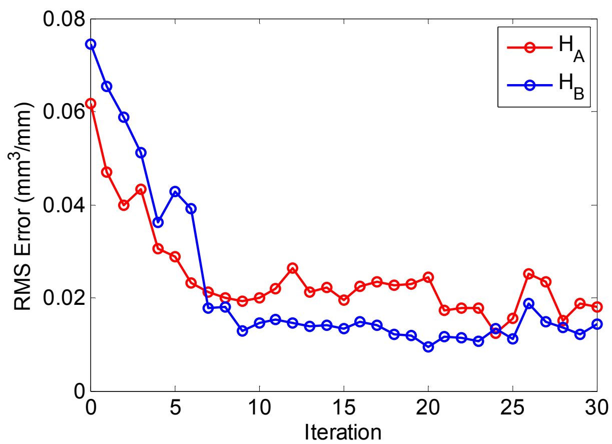

Fig. 4. Root mean squared error at each iteration for systems $H_A$ and $H_B$.

### B. *Signal Segmentation*

The control signals that yields the output responses seen in Fig. 3 are shown in Fig. 5. Notice that the more viscous Material B requires approximately 1.5 times the control effort to achieve approximately the same output as Material A. Each basis signal is demarcated by distinct transitions in signal magnitude that correspond to a particular basis task. The input signals for systems $H_A$ and $H_B$ are segmented at these demarcation points and stored as basis signals for their respective operation and system. Fig. 6 shows the input signal for system $H_A$ segmented into the constitutive basis signals. The input signal for system $H_B$ is segmented at the same points in time, not shown. The *Start*, *Stop*, and *Corner* basis signals are of finite length because each of these tasks occurs at a singular location. The *Steady-State* and *No-Flow* basis signals are of variable length because *Steady-State* and *No-Flow* regions are variable in length, as determined by the individual structure being constructed. The *Steady-State* signal is set to the mean input magnitude during the *Steady-State* region. The *No-Flow* signal is set to zero magnitude.

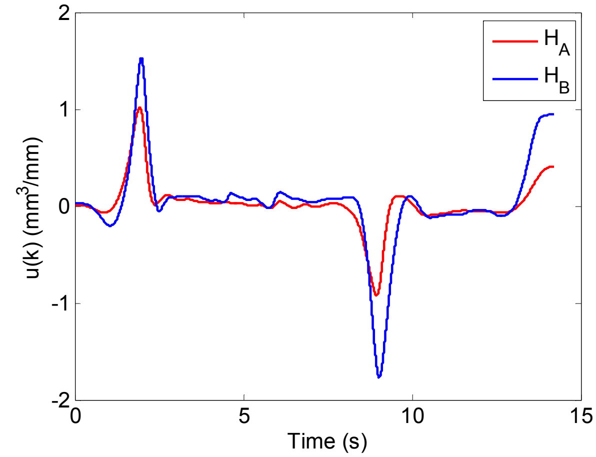


Fig. 5. Input signal $u(k)$ for iteration 31 for systems $H_A$ and $H_B$.

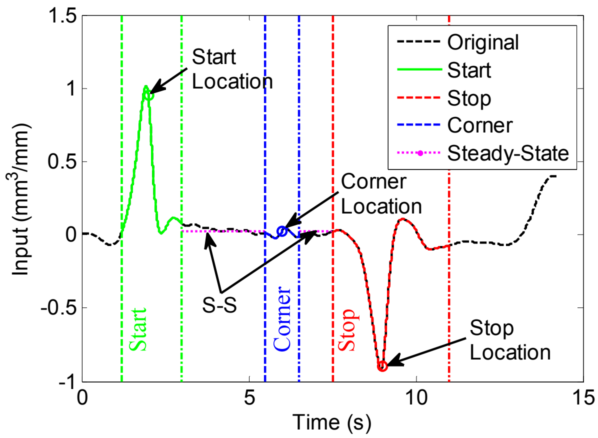


Fig. 6. Input signal $u_A(k)$ for iteration 31 for system $H_A$ segmented into its constitutive basis signals.

## C. Library Structure

The basis signals are assembled into matrix structure (3). Each basis signal is organized by task (*Start*, *Stop*, *Corner*, *Steady-State*, or *No-Flow*) and systems ($H_A$ or $H_B$) and numbered, 0, 1, …, $n$–1. Information critical to the signal extraction, Section IV, is contained in the first two rows of (3). $Lead_i$ informs the extraction algorithm how far in advance of the desired task the basis signal should begin. $K_i$ informs the extraction algorithm of the length of signal $u_i(k)$ for the specific basis task. The remaining rows contain the discrete time signals for each basis task, indexed by task number and time step.

$$\left\{ \begin{matrix} Lead_0 & Lead_1 & \cdots & Lead_{n-1} \\ K_0 & K_1 & & K_{n-1} \\ u_0(0) & u_1(0) & & u_{n-1}(0) \\ \vdots & \vdots & \ddots & \vdots \\ u_0(k) & u_1(k) & \cdots & u_{n-1}(k) \end{matrix} \right\} \tag{3}$$

# IV. Basis Signal Extraction

## A. Signal Selection

Basis signals from the control signal library, (3), are selected using logic applied to the computer language instructing the part construction. Three main considerations govern the logical decisions for extracting the correct basis signal: the current and future tasks, a hierarchy of tasks, and allowable task sequences.

### 1) Current and Future Tasks

The state of the current task and future tasks is continually monitored during a build operation. The control signal is generally non-casual, preempting the desired location of the task; therefore the extraction logic looks ahead in the computer language to determine the future tasks. Signals for the next task will begin as the current task is being completed.

### 2) Hierarchy of Tasks

In a given manufacturing application, some tasks assert priority over other tasks. In the case of µRD a *Stop* signal has the highest priority because of the possibility of short segments of material in which the *Start* and *Stop* signals will overlap in time. If the *Start* signal was allowed to complete and then followed by the *Stop* signal, the combination would result in excess material. Instead it is better terminate the *Start* signal short of completion, resulting in a less developed line of material. An analog of this hierarchical decision is with a pick-and-place robot system in which the pick operation would take highest priority so the robot will not miss items on an assembly line. A general hierarchy is shown in Fig. 7, where the highest priority task, task 0, is considered first followed by subsequent tasks in the hierarchy. In the case of µRD, the hierarchy is *Stop*, *Start*, *Corner*, *Steady-State*, and then *No-Flow*.

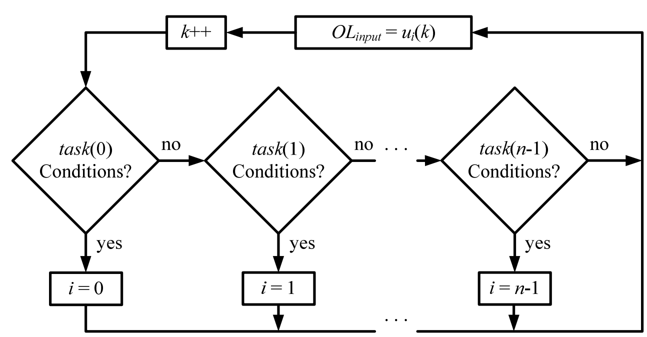


Fig. 7. Diagram of the hierarchy of tasks. The decision to select task 0 is considered first, followed by the subsequent tasks in the hierarchy. The open loop input signal, $OL_{input}$, is therefore a function of the active task and the time step within the selected signal.

### 3) Allowable Task Sequence

Integrated into the individual decision blocks in the task hierarchy are rules dictating which tasks are allowed to follow a previous task. For instance, the control signal cannot directly transition from the *Steady-State* signal to the *No-Flow* signal; a *Stop* signal must be executed first. Additionally, in a system switch, system $H_A$ must be stopped by its *Stop* signal followed by a dwell period to switch systems, and then by a *Start* signal for system $H_B$. An allowable tasks flow chart for a two material μRD system is shown in Fig. 8.

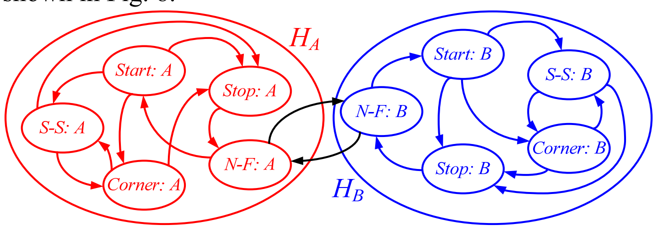


Fig. 8. Allowable tasks flow chart for a two material ($H_A$ and $H_B$) μRD system. Task changes within the same system are shown in their respective colors. Task changes that require a system switch are shown in black. (*S-S* = *Steady-State*, *N-F* = *No-Flow*).

## B. Signal Transfer

μRD characteristically has smooth signal transitions between the different tasks, reasonably satisfying *Assumption 4*. This characteristic simplifies the transfer of tasks because the transition will not excite high frequency dynamics in the system. The basis signals are simply sequenced without any signal modification at the transition. Not all applications will have this characteristic and measures to blend the two signals at the transition will need to be applied to satisfy *Assumption 4*.

## C. Basis Signal Extraction Example

Here we show an example sequence of basis signals applied to system $H_A$. In this simple example, the machine language commands the system to fabricate the structure in Fig. 9a. The signal extraction algorithm performs the logical operations described in Section IV to select both the next task in the sequence as well as to coordinate the timing based on information in the basis signal library. The sequence of basis signals to complete this operation is:

{*No-Flow, Start, Steady-State, Corner, Steady-State, Corner, Steady-State, Stop, No-Flow*}.

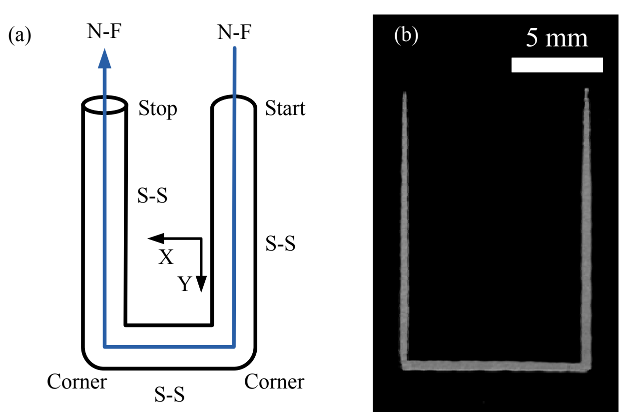


Fig. 9. Example of a sequence of basis signals used to construct a simple structure. (a) Schematic of structure. *S-S* = *Steady-State*, *N-F* = *No-Flow* (b) Image of structure after fabrication.

The appropriately sequenced basis signals, identified in Section III, are shown in Fig. 10. Basis signals *Steady-State* and *No-Flow* are interrupted at the appropriate time because they are outranked in the hierarchy by the *Start*, *Stop*, and *Corner* basis tasks. Notice the demarcation lines for beginning and ends of basis signals, as well as when in the signal the task is scheduled to happen. The resulting structure fabricated is shown in Fig. 9b.

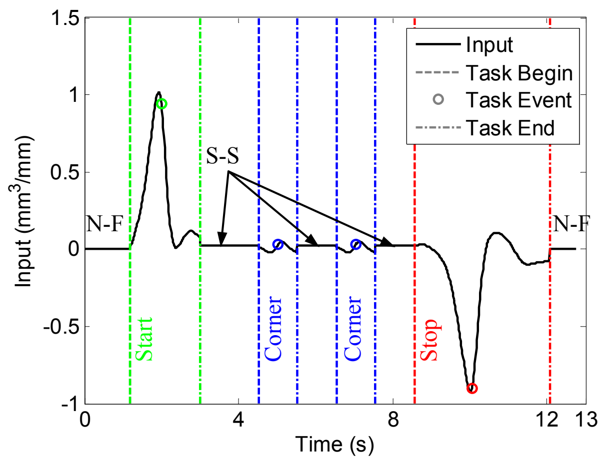


Fig. 10. Sequence of basis signals to build the structure in Fig. 9.

## V. Construction of Advanced Architectures

The basis signal approach to building a complete signal is best suited for advanced architecture structures that contain both multiple materials and frequent terminations and commencements in material deposition. These architectures either cannot be or are not easily learned in whole by ILC.

An example of a structure containing frequent terminations and commencements during material deposition is a tic-tac-toe structure, which has multiple linear and circular sections that are disconnected from each other. In this case, the entire operation could be learned in an extended identification procedure, however the process would be prohibitively time consuming and require extensive computational time to store and process image data. Here we build a tic-tac-toe structure, Fig. 11, from a sequence of the basis signals identified by the significantly reduced identification routine in Section III. Each task and its location are diagramed in Fig. 12. Note: the structure in Fig. 11 was fabricated with different basis signals than those shown in Fig. 10, however basis signals used were identified with a method identical to Section III.

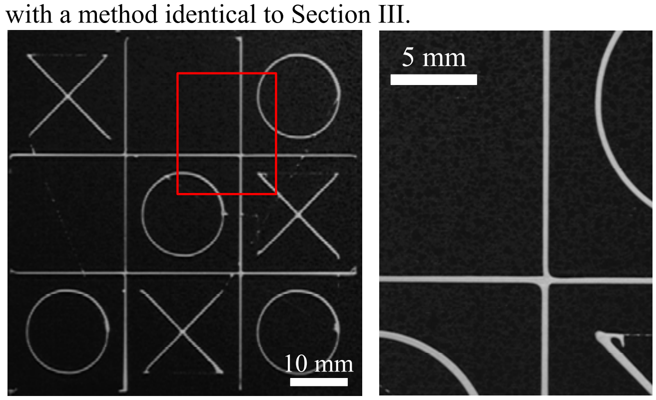


Fig. 11. Tic-tac-toe structure exhibiting the ability to perform all five tasks, *Start*, *Stop*, *Corner*, *Steady-State*, and *No-Flow*. Image on the right is an enlarged section of complete structure, denoted by the red box in the left image.

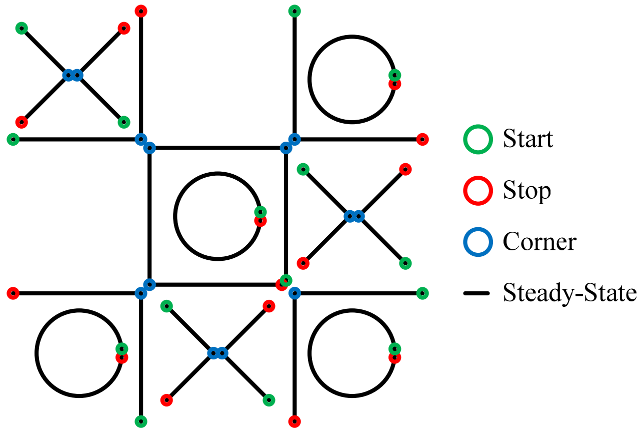


Fig. 12. Diagram of tasks to build the tic-tac-toe structure in Fig. 11.

## VI. Conclusions

ILC is an effective algorithm for improving system performance on many systems that track repetitive trajectories. However, ILC is traditionally trajectory specific. This paper explores a modular approach to ILC, exploiting the repetition of tasks that is common to manufacturing operations. By applying signals learned through ILC as modular basis signals, system unfit for traditional ILC, such as those requiring abrupt changes in system dynamics and lengthy trajectories, can be controlled. The process of implementing this approach is displayed on a multi-material μRD system, a system that has multiple system dynamics depending on the material being deposited and typically requires lengthy build times. The identification, segmentation, and storage of basis signals corresponding to a set of basis tasks is displayed, as well as the algorithm for extracting basis signals depending on machine language governing structure fabrication. An example of an advanced architecture structure, containing multiple repetitions of basis tasks, is displayed. The total build time in this example is prohibitively long for conventional implementations of ILC, but by using the basis signal method introduced here, the structure can be fabricated with a significantly decreased ILC identification.

## Acknowledgment

The authors acknowledge Dr. Tay Bee Yen and Dr. Lin Wei at the Singapore Institute of Manufacturing Technology (71 Nanyang Drive, Singapore 638075) for their help with the design and manufacture of the Multi-Material Deposition Head.

## References

1 Bristow, D.A., Tharayil, M., and Alleyne, A.G., "A Survey of Iterative Learning Control," *IEEE Control Systems Magazine*, pp. 96-114, 2006.

2 de Roover, D. and Bosgra, O.H., "Synthesis of Robust Multivariable Iterative Learning Controllers With Application to a Wafer Stage Motion System," *International Journal of Control*, vol. 73, no. 10, pp. 968-979, 2000.

3 van de Wijdeven, J. and Bosgra, O., "Hankel Iterative Learning Control for Residual Vibration Suppression with MIMO Flexible Structure Experiments," *Proceedings of IEEE American Control Conference 2007,* 2007.

4 Lee, J.H., Lee, K.S., and Kim, W.C., "Model-Based Iterative Learning Control With a Quadratic Criterion for Time-Varying Linear Systems," *Automatica*, vol. 36, no. 5, pp. 641-657, 2000 .

5 Hoelzle, D.J., Alleyne, A.G., and Wagoner Johnson, A.J., "Iterative Learning Control for Robotic Deposition Using Machine Vision," pp. 4541-4547, 2008.

6 Cesarano, J., Segalman, R., and Calvert, P., "Robocasting Provides Moldless Fabrication From Slurry Deposition," *Ceramic Industry*, vol. 148, no. 4, pp. 94-102, 1998.

7 Han, W., Jafari, M.A., Danforth, S.C., and Safari, A., "Tool Path-Based Deposition Planning in Fused Deposition Processes," *Transactions of the ASME: Journal of Manufacturing Science and Engineering*, vol. 124, pp. 462-472, 2002 .

8 Lewis, J.A., Smay, J.E., Stuecker, J., and Cesarano III, J., "Direct Ink Writing of Three-Dimensional Ceramic Structures," *Journal of the American Ceramic Society* , vol. 89, no. 12, pp. 3599-3609, 2006.

9 Lewis, J.A., "Direct Ink Writing of 3D Functional Materials," *Advanced Functional Materials*, vol. 16, pp. 2193-2204, 2006.

10 Smay, J.E., Cesarano III, J., and Lewis, J.A., "Colloidal Inks for Directed Assembly of 3-D Periodic Structures," *Langmuir*, vol. 18, no. 14, pp. 5429-5437, 2002.

11 Zesch, W., Brunner, M., and Weber, A., "Vacuum Tool for Handling Microobjects With a Nanorobot," *Proceedings of the 1997 IEEE International Conference on Robotics and Automation,* pp. 1761-1766, 2007.

12 Bristow, D.A. and Alleyne, A.G., "A High Precision Motion Control System With Application to Microscale Robotic Deposition," *IEEE Transactions on Control Systems Technology*, vol. 14, no. 6, pp. 1008-1020, 2006.

13 Han, W. and Jafari, M.A., "Coordination Control of Positioning and Deposition in Layered Manufacturing," *IEEE Transactions on Industrial Electronics*, vol. 54, no. 1, pp. 651-659, 2007.

14 Bellini, A., Güçeri, S., and Bertoldi, M., "Liquefier Dynamics in Fused Deposition," *Journal of Manufacturing Science and Engineering*, vol. 126, pp. 237-246, 2004.

15 Hoelzle, D.J., "Reliability Guidelines and Flowrate Modulation for a Micro Robotic Deposition Systems," Masters Thesis, University of Illinois at Urbana-Champaign, Urbana, IL, 2008.